[Supplementary material]

Summary justice or the King's will? The first case of formal facial mutilation from Anglo-Saxon England

Garrard Cole[1,*], Peter W. Ditchfield[2], Katharina Dulias[3,4], Ceiridwen J. Edwards[2,3], Andrew Reynolds[1] & Tony Waldron[1]

[1] *Institute of Archaeology, University College London, UK*

[2] *Research Laboratory for Archaeology, School of Archaeology, University of Oxford, UK*

[3] *Department of Biological and Geographical Sciences, University of Huddersfield, UK*

[4] *Department of Archaeology, University of York, UK*

[*] *Author for correspondence: ✉ tcrngco@ucl.ac.uk*

Osteological analysis

The osteological analysis was carried out using standard methods (outlined in Ferembach *et al*. 1980; Buikstra & Ubelaker 1994). The basis behind the methods was to use as many age and sex variable factors as possible. The limited material in this case restricted analysis to cranium morphology, suture fusion, dental development and tooth wear.

Taphonomic considerations

The cranium in question was found in an unclean state in the Hampshire Cultural Trust stores. This turned out to be fortunate for two reasons; firstly, it allowed excavation damage to be excluded as a cause for crucial changes to the facial area (as detailed below); secondly, it allowed the otherwise poorly recorded material to be associated with a specific distinctive archaeological feature, which served to explain the taphonomic changes observed on part of the exterior surface.

The cranium as found was covered in a very fine dark silt sediment with no sign of any chalk inclusions as were reported in almost all archaeological features observed during the excavations. The silt totally filled all tooth sockets, with the exception of a solitary *in-situ* left first maxillary molar. The nasal aperture was also completely filled with a thin layer of sediment, masking the face, especially between the anterior nasal spine and prosthion (or rather where the prosthion would have been).

The exterior surface showed variable irregular surface degradation, more pronounced on the occipital bone. The endocranial surface was generally in very good condition. The

unmodified bone surface was coloured a medium orange brown, whilst the degraded surface was lighter in colour. The surface taphonomy changes are consistent with partial exposure in a wet environment. The right temporal bone was not recovered. The sharp well-defined appearance of the zygomatic part of the right zygomatico-temporal suture suggests the loss of the temporal occurred shortly before recovery from the spoil heap.

Age at death estimation

The human skeleton and dentition undergoes changes associated with age. Age-dependent factors include dental development and eruption, long bone diaphysis length, long bone epiphyseal fusion, cranial suture fusion and changes to the morphology of the pelvis, specifically the auricular surface and the pubic symphysis. For some populations known to have had an appropriate diet, wear of the occlusal surface of the teeth may also be used. One complicating factor is the sex-dependent nature of some of these changes. The error ranges on the age estimates increases significantly with age. The primary age-at-death indictors were the state of development of the few teeth present and the status of some cranial sutures and synchondroses. The cranium was clearly that of a young person, as the maxillary third molars were just erupting from their crypts (Figure S1). The only *in-situ* erupted tooth was a left first maxillary molar. The tooth was lightly worn, with loss of cusp enamel, but the crown was otherwise complete, apart from a small chip at the mesio-buccal corner.

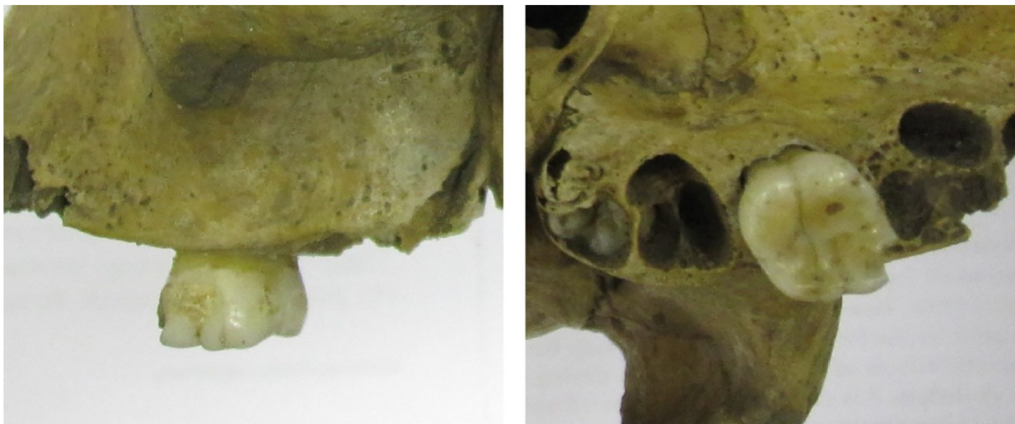

Figure S1. Upper left M1 tooth in-situ in maxilla, showing occlusal and buccal views.

There appeared to be a taphonomic linguo-buccal fissure running through the crown and slight amounts of dental calculus. This sole molar was extracted for dietary and locational stable isotopic analysis, revealing fully developed roots. An X-ray showed that the sockets for the second molars were as deep as those of the first molars, suggesting that the second

molar was also fully developed. The third molars were visible in the maxilla, but had not erupted. The third molars had fully developed crowns with roots some way between quarter and half development. All other sockets were present but with the relevant teeth lost post-mortem. Dental development data (Moorrees *et al*. 1963; Al Qahtani 2008) suggests a developmental age at death of 15±3 years. The utility of dental formation for estimating developmental age (Moorrees *et al*. 1963) has been validated by Saunders *et al*. (1993). The method strictly only applies to mandibular dentition, but it is applicable to the maxillary permanent molars as the developmental stages closely match (Al Qahtani 2008; Al Qahtani et al. 2014).

Miles (1962) developed techniques for determining age at death based on tooth wear. He used a high tooth wear population from the Anglo-Saxon period as his reference, so the method is applicable here. The pattern of occlusal wear on the first molar suggests a range of 18±3 years.

Cranial suture fusion has a long history for age at death estimation (Broca 1868), but in spite of recent attempts to improve its utility (Alhazmi *et al*. 2017), still tends to be used as an indicator of last resort. The state of cranial suture fusion is listed in Table S1.

Table S1. Fusion status of the cranial sutures.

Suture	Fusion state
Metopic	Fused, not visible
Nasal	Fusing
Sagittal	Fusing
Coronal	Fusing
Occipito-mastoid	Unfused
Lambdoid	Unfused
Parieto-temporal	Unfused
Zygomatico-temporal	Unfused

The basal occipito-sphenoidal synchondrosis was unfused, though the surface morphology suggested that fusion was in progress. Data from Alhazmi *et al*. (2017) suggests the individual had a developmental age at death in the range 10–20 years.

Biological sex assessment

The human skeleton exhibits some degree of sexual dimorphism. This can be used, with appropriate caveats, to assess the biological sex of the individual. Skeletal dimorphism starts

to be expressed during puberty and becomes clearest in early adulthood. However, older females may develop changes to the skull normally associated with males, and so age has to be taken into account when assessing sex. The primary data for assessment comes from skull morphology, pelvis morphology and long bone metrics. In this case, cranium morphology was the sole source of data.

The cranium had rounded features, with prominent frontal bossing, a gracile zygomatic arch, and a sharply-defined supra-orbital margin. The maxilla was very broad in relation to its antero-posterior length. The mastoid process was short but rather broad in the antero-posterior direction. Superficial surface degradation had removed the fine detail of the exterior surface of the occipital bone, but it appeared to lack prominent muscle attachments. The temporal ridge was also smooth. These features suggest the individual was possibly female.

Trauma

Cleaning of the cranium revealed clear evidence of peri-mortem trauma (Figure 2). First, there was a linear cut on the medial left frontal bone with a v-shaped profile, oriented obliquely to the right when facing the cranium. Second, the removal of sediment revealed exposed trabecular bone at the base of the nasal aperture, cutting through the front of the maxillary central incisor sockets. The anterior nasal spine was also missing. The trabecular zone was surrounded by a margin of sharply defined cortical bone, especially at the base of the nasal aperture. The lower left and right lateral margins of the nasal aperture were also truncated. These features mark the trauma as peri-mortem, though it is not clear whether the event happened before death or shortly afterwards whilst the bone was still fresh.

Overall, there appeared to be one or more straight cuts through the nasal margin from midway up the nasal aperture through the anterior nasal spine to the prosthion. The cuts removed the anterior nasal spine and the area in proximity to prosthion. Close examination of the lateral aspect revealed a sharp v-shaped nick on the left side of the nasal aperture, with the cut through the lips at a slightly different angle to that through the nasal margins. The direction of inclination of the cuts is consistent with a right-handed opponent facing the victim.

Ethnicity

Cranial morphology may give some clue as to the ethnicity of regional origin of an individual, and there are general trends of shape thought to broadly distinguish major regional groups, such as European, Asian, African and Native American. However, there is

considerable overlap between the skull shapes for these regions, and any such assessment serves only as a guide. The analysis is usually performed via a multidimensional discriminant analysis of metrical data for the skull (or cranium) in question. Fordisc (ver. 3.1; Jantz & Ousley 2005) is the best known and most widely used implementation of this approach. The measurements are made between pairs of well-defined anatomical landmarks, with each measurement identified by a distinct three-letter code. The resultant data set is tested against reference populations of skulls of known ancestry. The program produces a list of matching skulls, matched according to minimum multidimensional geometric distance.

The metric data for the Oakridge cranium is listed in Tables S2 and S3. The data marked as 'estimate' could not be obtained directly as the relevant area on one side of the cranium was damaged. The data was estimated measuring from the centre line to the good side and doubling the result.

Table S2. Metric data for the Oakridge cranium ordered by measurement reference code. The data is rounded to the nearest millimetre. Key: * - estimates based on unilateral measurements from the centre line to the side where the landmark is present; ** - estimate based on projected location of prosthion.

Code	Metric (mm)
ASB	105
AUB	118
BBH	127
BNL	96
DKB	21
EKB	91
FMB	91
FOB	27
FOL	35
FRC	103
FRS	27
GOL	169
JUB	107
MAB	61
NLB(**)	23
NLH	45

Code	Metric (mm)
NOL	166
NPH	61
OBB	38
OBH	32
OCC	92
PAC	102
PAS	23
STB	111
WCB	75
WMH	21
WNB	12
XCB	126
XFB	112
ZYB(*)	117
ZMB	86

Table S3. Fordisc results showing primary and secondary matched groups with associated probabilities for various subsets of the measured data in Table S2.

Measurement dataset	Reference Database	Primary match		Secondary match	
		Group	Probability	Group	Probability
all measurements included	modern forensic database	Hispanic female	0.659	African female	0.201
all measurements included	Howell's database	Zalavar (Hungary) female	0.52	20thC white female	0.211
only ZYB measurement included	modern forensic database	Black female	0.502	Hispanic female	0.362
only ZYB measurement included	Howell's database	Zalavar (Hungary) female	0.373	Atayal (Taiwan) female	0.308
both NLB and ZYB measurements excluded	modern forensic database	Black female	0.457	Hispanic female	0.269
both NLB and ZYB measurements excluded	Howell's database	Zalavar (Hungary) female	0.448	Atayal (Taiwan) female	0.396

Discussion

The nature of the taphonomic changes present on the posterior and right endocranial surface of the cranium, in combination with the presence of very fine silt in the orbital, nasal and alveolar regions, suggested that the cranium was recovered from a watery environment (Knüsel & Carr 1995).

Given the limited data and the relatively poor accuracy of the ageing methods available, it was only possible to provide a relatively broad estimate for the age of death of the individual. Taken in combination, the age determination features indicated that the individual was certainly not adult at the time of death, and possibly had a developmental age of around 15–18 years.

The cranial morphology was typically female, but young males may also exhibit such features prior to full expression of sexual dimorphic traits. Given the young age of the individual, and the absence of the pelvis, it was not possible to confidently determine the sex of the individual on the basis of morphological traits alone.

There was clear evidence for perimortem trauma to the frontal bone and the facial region. The fact that the cut marks only appeared after removal of residual sediment from the cranium allows excavation damage to be excluded as a cause. In addition to the oblique cut on the frontal bone, it appeared that at least two further cuts were made to inflict the injuries (Figure 4). The narrow nature of all these features suggested a narrow sharp bladed instrument, such

as a knife or seax was used, rather than a sword or a broader bladed implement such as an axe (Lewis 2008). The cuts in the nasal area are consistent with a knife blade slicing through the nasal soft tissue and that of the upper lip sufficiently deeply to cut through the thin cortical bone. If the wounds were made before death, the presence of multiple wounds in the facial region suggests deliberate intent rather than fortuitous blows. In this case, it is likely that the individual was restrained in some manner. In the absence of other parts of the skeleton, it is not possible to say anything about trauma elsewhere on the body, and so we cannot determine the mode of death. The trauma may also have been inflicted, in part or in whole, after the individual had died, whilst the bone was still in fresh condition.

The norma frontalis view of the cranium exhibits some distinctive features – a large intra-orbital breadth, rectangular orbits and a nasal aperture very broad in relation to its height. The use of Fordisc to investigate possible ethnicity has known limitations (Ramsthaler *et al*. 2007; Elliot & Collard 2009), And the problems are more pronounced in archaeological specimens, arising from taphonomic modification of skull morphology, potential masking of reference landmarks, and post-burial shape deformation. However, the facial area of this individual was well preserved. Other areas exhibited variable surface bone loss, which will have inevitably affected measurements. The results using the forensic data show great variability of association, according to which estimated data values are used. The program also showed that most measured data values fell within one or two standard deviations below the dataset mean values. This is not surprising given the young age of the individual. The comparisons with Howell's dataset (Howells 1973, 1989) were more consistent, preferring an association with the Zalavar (Hungary) female throughout. However, with one exception, the probability associated with the primary preference was around 0.5 or less. These results do not permit any statement about potential ethnic origin to be made with any confidence. The genetic analysis discussed below offers a more definitive answer to this question.

Radiocarbon dating

A powdered sample was extracted from the inner table of the occipital bone in order to determine a radiocarbon date for the specimen. Sub-sampling was carried out by Tom Higham at the Oxford Radiocarbon Laboratory. The surface of approximately 1cm square of the inner table was cleaned using 5µm aluminium oxide abrasive powder in an environmental cabinet. A high speed drill was then used to extract around 100mg of bone powder. This was processed using the standard Oxford Laboratory protocol (Bronk Ramsey *et al*. 2002, 2004a, 2004b).

The sample was assigned dating code OxA-26646 and the uncalibrated date was determined to be 1173 BP with an error of ±24 years. This date was calibrated using OxCal (ver. 4.1.7; Bronk Ramsey 2017) and the most recent calibration curve, IntCal 13 (Reimer *et al*. 2013). The calibrated date was determined to be between AD 776-899 (87.3%) and 920- 946 (8.1%) at 2σ (95.4%) (Figure S2). The mean date was AD 846 and the median date was AD 843. Stable isotopic evidence (see below) suggested that there was no significant marine component to the diet of this individual, and, therefore, the date did not require a marine correction.

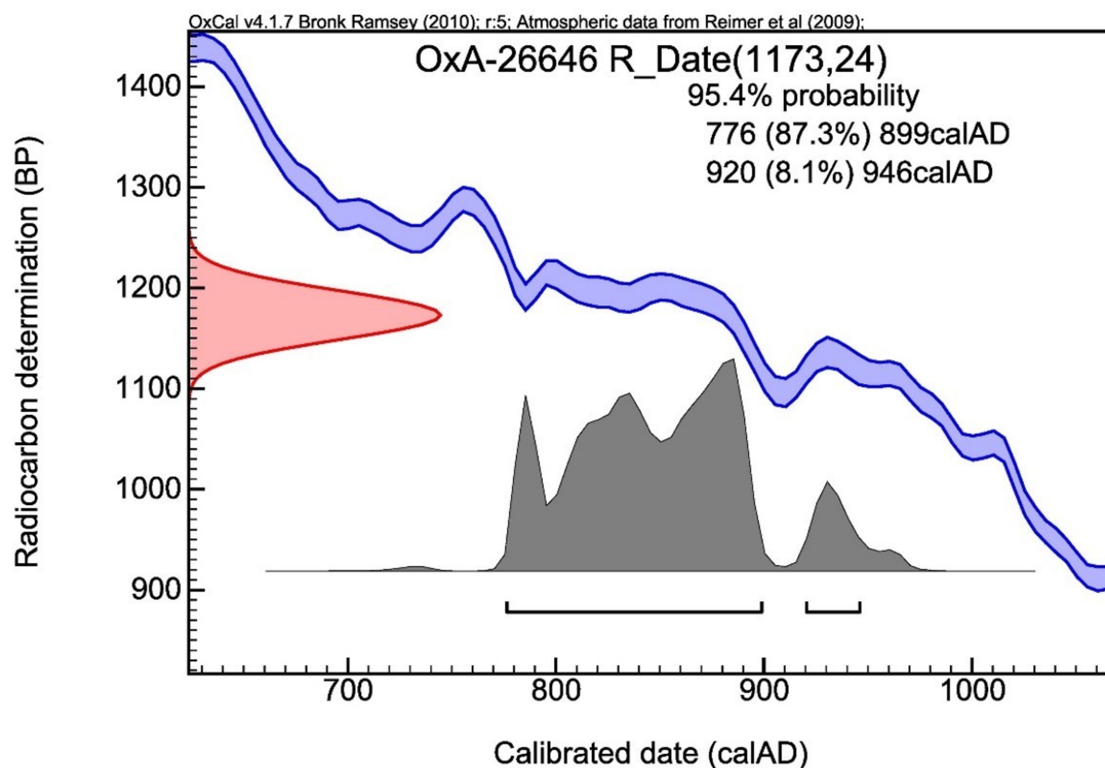

Figure S2. Calibrated radiocarbon dates for the Oakridge individual based on an uncalibrated date of 1173±24 years BP (using OxCal v4.17 and IntCal13; Reimer et al. *(2009); Bronk Ramsey (2010)).*

Although the date of late eighth to ninth century AD (between cal AD 776 and 946) encompasses the documented Battle of Basing, which occurred between Danes and local Saxons on the 22 January AD 871 (King & Cole 2016), there is nothing to suggest that this isolated burial is related to that event.

Stable isotopic analysis

The left maxillary first molar was selected for carbon (C), nitrogen (N), oxygen (O) and strontium (Sr) stable isotopic analyses at the Research Laboratory for Archaeology at the University of Oxford (England).

Dental enamel strontium measurement

The tooth crown was cleaned in an ultrasonic bath of deionised water for three minutes. The area selected for enamel sampling was then surface abraded with 5µm aluminium oxide powder using a compressed air abrasive system. 20mg of enamel powder was extracted from the buccal surface using a diamond impregnated dental burr. Sample dissolutions were performed following the method of Cohen *et al*. (1988). Samples were dissolved in PFA (polyfluroalkoxy) beakers on a hot plate (*c*. 150°C, 24 hours) in a 7:3 mixture of 29M HF and 14M HNO_3. Samples were repeatedly evaporated to dryness and the residue re-dissolved in 14M HNO_3. Strontium was separated by the method described by Míková & Denková (2007), which is a development of the method described by Pin *et al*. (1994). This is a variation of the standard ion exchange method, in this case using Sr. Spec ion exchange resins obtained from Eichrom Environment (Bruz, France) (see Míková & Denková 2007 for details).

All Sr isotopic analyses were performed on a Nu Instruments NuPlasma HR in the AEON EarthLAB, housed in the Department of Geological Sciences, University of Cape Town, Rondebosch, South Africa. Extracted Sr samples were analysed as 200ppb in 0.2% HNO_3 solution, using NIST SRM987 as a reference standard (mean value of 0.710302, n = 8, and 2 sigma = 0.000027, where the internationally agreed reference value equals 0.710255). All Sr isotope data were corrected for rubidium (Rb) interference using the measured signal for ^{85}Rb and the natural $^{85}Rb/^{87}Rb$ ratio. Instrumental mass fractionation was corrected for using the exponential law and an $^{86}Sr/^{88}Sr$ value of 0.1194.

Dental enamel oxygen and carbon measurements

Two milligrams of the untreated enamel from the tooth was used for oxygen stable isotopic analysis. This was pre-treated with 1M CH_3COOH solution for three hours at room temperature to remove any secondary carbonates and then rinsed to neutrality with deionised water and freeze dried prior to isotopic analysis. The sample was analysed for $\delta^{13}C$ and $\delta^{18}O$ using a VG Isogas Prism II mass spectrometer with an on-line VG Isocarb common acid bath

preparation system, where it was reacted with purified phosphoric acid (H_3PO_4) at 90°C. The evolved CO_2 was pre-concentrated using a cold finger apparatus prior to admission to the dual inlet system on the mass spectrometer. Calibration to V-PDB standard was via NBS-19 using the Oxford *in-house* (NOCZ) Carrara marble standard. The replicate values for the *in-house* standards run with the sample in this study gave a mean value of 2.96‰ for $\delta^{13}C$ with a standard deviation of 0.022, and a mean value of -1.91‰ for $\delta^{18}O$ with a standard deviation of 0.026 (n = 8). Expected values for the *in-house* standard were 2.307‰ for $\delta^{13}C$ and -1.906‰ for $\delta^{18}O$ relative to V-PDB.

Mammalian tooth enamel contains up to 2% carbonate anions substituted for phosphate anions within the hydroxyapatite matrix of the enamel. The carbon and oxygen isotopic values of tooth enamel carbonate (referred to as $\delta^{13}Cc$ and $\delta^{18}Oc$, respectively) were measured to try to determine the location at which the Oakridge individual was living at the time the enamel was being formed. The value of $\delta^{18}Oc$ will be related to the oxygen isotopic value of the local drinking water (referred to as $\delta^{18}Ow$) (Pollard & Heron 2008: 371) and this, in turn, is thought to reflect the oxygen isotopic value of local rainfall (although significant use of ground water as a drinking water source will modify this signal somewhat). The tooth enamel carbonate carbon isotopic value ($\delta^{13}Cc$) will be related to the blood bicarbonate reservoir and, as such, reflects total diet.

The $\delta^{13}Cc$ and $\delta^{18}Oc$ values were measured relative to the international standard V-PDB scale. However, to arrive at a likely oxygen isotopic composition for drinking water, several transformations had to be made. Firstly, the $\delta^{18}Oc$ values were converted from the V-PDB scale to the SMOW-SLAP (Standard Mean Ocean Water- Standard Light Antarctic Precipitation) scale using the equation of Kim *et al*. (2015):

$$\delta^{18}O\ (SMOW) = 1.03091 \times \delta^{18}O\ (V\text{-}PDB) + 30.91$$

The $\delta^{18}Oc$ values measured in carbonate were then converted into an estimated value phosphate fraction equivalent, $\delta^{18}Op$ for comparison with published values, using the equation of Bryant *et al*. (1996):

$$\delta^{18}Op = (\delta^{18}Oc - 8.3)/1.02‰$$

Finally, a theoretical value for the oxygen isotopic composition of the drinking water available at the time of tooth enamel mineralisation, $\delta^{18}Ow$, usually assumed to be equivalent to local rain water values, was calculated using the equation of Levinson *et al*. (1987):

$$\delta^{18}Ow = (\delta^{18}Op - 19.4)/0.46$$

Dietary stable isotope analysis

Collagen for carbon and nitrogen stable isotopic analysis was prepared from the dentine of the tooth crown. The sample was demineralised using 10ml aliquots of 0.5M HCl solution at 4°C. The acid was changed at 48 hour intervals until no further reaction was seen. The sample was then rinsed three times with milli-μ ultra-pure water and placed in 10ml of pH3 water at 75°C for 48 hours. The sample was filtered using an Eezee™ filter, and the supernatant liquid decanted into a Nalgene™ tube with a temporary Parafilm™ cover. The sample was pre frozen at -40°C prior to freeze drying in a Zirbus VaCo5 freeze drier fitted with an oil free vacuum system for 72 hours.

The resulting purified collagen was weighed out for analysis using *c*. 1mg aliquots weighed into pre-cleaned tin capsules. Samples were combusted on a Sercon GSL elemental analyser system using a helium carrier gas with a flow of approximately 80ml per minute. A 2% split of the gases evolved was analysed for nitrogen and carbon stable isotopic composition using a Sercon -20/22 gas source mass spectrometer. Isotopic values, as well as elemental abundances and carbon-to-nitrogen ratios, were calibrated against an Oxford *in-house* alanine standard, which itself is routinely measured against international standards (USGS 40 and USGS 41 glutamic acid, whose values are traceable back to the V-PDB and AIR international standards for carbon and nitrogen, respectively). Further aliquots of the alanine standard were used to monitor and correct for instrumental drift. The sample was run in triplicate. Stable isotopic results were reported in delta notation relative to V-PDB for carbon and AIR for nitrogen. Replicate analysis of the alanine *in-house* standard gave the following results (n = 10 measurements): mean $\delta^{13}C$ = −27.15±0.13‰, expected value −27.11‰; mean $\delta^{15}N$ = −1.55±0.15‰, expected value −1.56‰. This suggests that the individual values obtained during the analyses reported here are typically accurate to better than ±0.1‰ for both $\delta^{13}C$ and $\delta^{15}N$.

Results

The isotopic results from the sample analysed in this study are given in Table S4. The collagen prepared from the tooth dentine gave a C/N ratio of 3.1, suggesting that the collagen was well preserved and likely to give a good measure of the *in-vivo* dietary carbon and nitrogen stable isotopic values (van Klinken 1999). The collagen prepared from the dentine fraction of the tooth gave a $\delta^{15}N$ value of 11.71‰ relative to AIR, and a $\delta^{13}C$ value of −19.03‰ relative to V-PDB, both with error of ±0.2‰. The tooth enamel carbonate fraction

of the sample gave δ^{13}Cc value of −12.78‰ ±0.01 and a δ^{18}Oc value of −6.47±0.02 both relative to V-PDB. Tooth enamel also gave an $^{87}/^{86}$Sr ratio of 0.710279±0.000014.

Table S4. Stable isotopic data from Oakridge individual.

Tooth sampled	Tissue type	C:N ratio	δ^{15}N (AIR)	δ^{13}C (V-PDB)	δ^{13}Cc (V-PDB)	δ^{18}Oc (V-PDB)	δ^{18}Op (VSMOW)	$^{87/86}$Sr
ULM1	dentine	3.1	11.71	-19.03	---	---	---	---
ULM1	enamel	n/a	---	---	-12.778	-6.471	24.239	0.7103

Discussion

The calculated δ^{18}Ow value for the tooth enamel in this study was −9.22‰ SMOW, whereas modern ground water δ^{18}O values for the area where the sample was found are around −7‰ SMOW (Darling & Talbot 2003). The conversion of measured carbonate values to theoretical phosphate values, and thence to probable water values, is fraught with uncertainty regarding the factors in the equations used to make the conversions (see Pollard *et al*. 2011 for discussion). However, in this instance, there seems to be sufficient difference between the likely drinking water composition at the time of tooth mineralisation, and the modern ground water composition at the location where the sample was excavated, to suggest that this individual was probably non-local.

The strontium isotopic composition of tooth enamel is strongly influenced by the underlying geology at the time of tooth mineralisation (Bentley 2006; Chenery *et al*. 2010). The underlying bedrock geology of the site area is upper Cretaceous chalk of the Seaford Chalk Formation, with typical $^{87/86}$Sr ratios of between 0.708 and 0.709 (Evans *et al*. 2010). However, the site lies relatively close to the boundary of the overlying Tertiary rock of the Lambeth Group and the London Clay Formation, which have typical $^{87/86}$Sr ratios of between 0.709 and 0.710 (Evans *et al*. 2010). The tooth enamel $^{87/86}$Sr ratio value measured from the Oakridge individual was 0.710279±0.000014, which falls well outside of the range for the local chalk and just outside of the range for the nearby Tertiary sediments. This also suggests that this individual was probably not local; that is, she did not spend her early years, during the time of M1 mineralisation, in the immediate area around Basingstoke.

The dentine collagen carbon and nitrogen stable isotopic results, of δ^{13}C −19.03‰ (V-PDB) and δ^{15}N of 11.71‰ (AIR), respectively, suggest a predominantly terrestrial diet with a minor marine protein component. However, in the absence of any associated faunal remains from the same location, it is impossible to give an absolute indication of what these values might

mean in terms of the relative amounts of plant versus terrestrial animal versus marine protein consumed. Comparable local dietary isotopic data sets are available from Worthy Park near Winchester, Hampshire (approximately 25 kilometres southwest of Basingstoke), and Alton, Hampshire (around 15 kilometres to the southeast) (Hull 2008). These sites have yielded mean $\delta^{13}C$ values for adult human bone collagen of −20.38‰ and −20.51‰, with a standard deviation of 0.35 (n = 26) and 0.26 (n = 25) respectively, and mean $\delta^{15}N$ values of 8.59‰ and 9.11‰, with a standard deviation of 1.15 (n = 26) and 0.70 (n = 25), respectively. By comparison, the values for the Oakridge individual are higher in both $\delta^{13}C$ and $\delta^{15}N$ than the means reported for the Worthy Park and Alton Saxon burials (Figure S3).

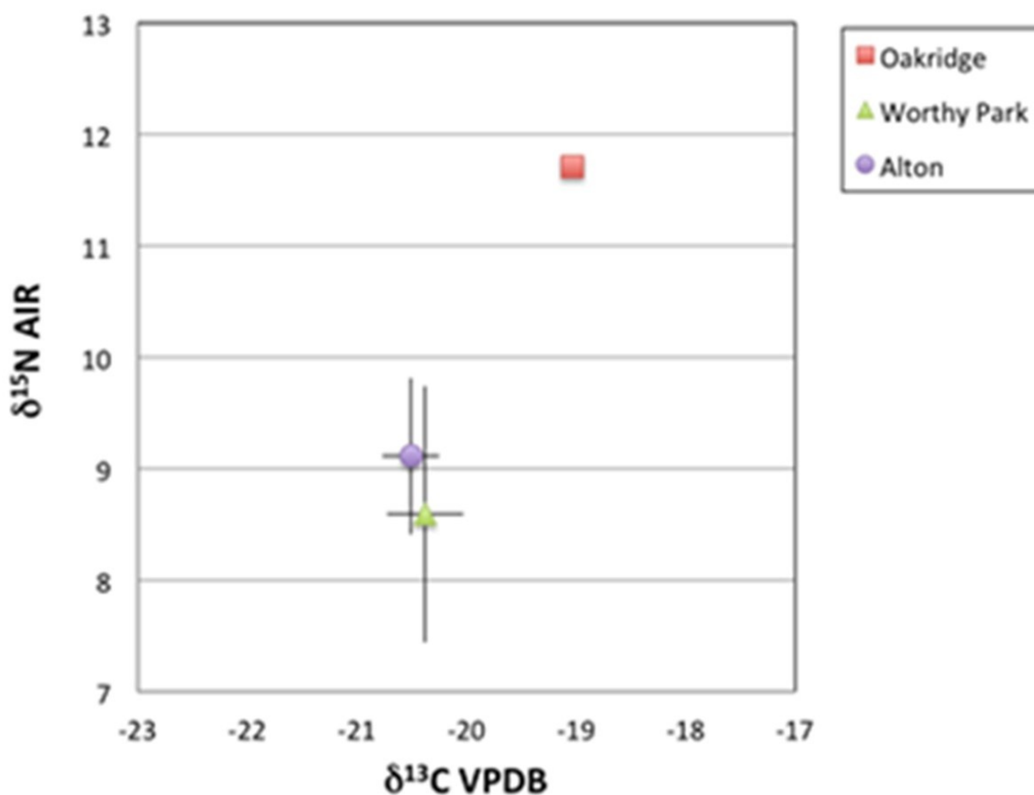

Figure S3. Oakridge collagen stable isotopic composition compared to two other inland human assemblages from Hampshire (Hull 2008).

This suggests that the diet of the Oakridge individual was slightly anomalous compared to the average diet that might be expected for inland Hampshire in middle Saxon times, with the less negative value for $\delta^{13}C$ and the more positive value for $\delta^{15}N$ suggesting more of a marine component in the Oakridge diet than usual for inland Hampshire. Taken alongside the strontium and oxygen isotopic data, the dietary stable isotopic information is also compatible with a probable non-local origin for this individual.

Ancient DNA analysis

Sampling and extraction

The same left maxillary first molar that had been selected for the stable isotopic analyses was also sampled for ancient DNA. Sample processing was done at the Ancient DNA Facility of the University of Huddersfield (England) under dedicated clean-room conditions supplied by a positive air pressure system. Full body suits, hairnets, gloves and face masks were worn throughout the sampling, extraction and library preparation processes. All tools and surfaces were constantly cleaned with bleach, LookOut® DNA Erase (SIGMA Life Sciences), as well as with ethanol and long exposures to UV light.

The surface of the tooth root was decontaminated by UV radiation for 30 minutes on each side, followed by cleaning with 5µm aluminium oxide powder using a compressed air abrasive system. The root was removed using a diamond-tipped cutting saw attached to a hobby drill, and this was then shaken with a steel ball inside a metal shaker in a Mixer Mill (Retsch MM400) for 30 seconds at 30Hz frequency. DNA was extracted from approximately 150mg of the sample tooth root powder produced, following the protocol by Yang *et al*. (1998) with modifications by MacHugh *et al*. (2000). Blank controls were included throughout the sampling procedure, extraction and library preparation to allow for estimation of possible modern DNA contamination.

Library preparation

Next-generation sequencing libraries were constructed from DNA extracts using the methods by Meyer & Kircher (2010) and Kircher *et al*. (2012), with modifications outlined in Gamba *et al*. (2014) and Martiniano *et al*. (2014). All DNA purification steps were performed using the QIAQuick MinElute purification kit (Qiagen) following the manufacturers protocol, with the modification of adding 0.05% Tween 20 (Fisher BioReagents) to the Elution Buffer. Three dual-indexed libraries were prepared for this sample as follows.

After treatment with USER (Uracil-Specific Excision Reagent) enzyme (NEB) for 3 hours at 37°C, the sample DNA underwent blunt-end repair step using NEBNext® End Repair Module (NEB) for 15 minutes at 25°C followed by 5 minutes at 12°C. The sample was cleaned using a QIAQuick MinElute PCR purification kit (Qiagen), and then adapter ligation was performed using T4 DNA polymerase buffer (Thermo Scientific) at 22°C for 30 minutes. After another QIAQuick purification step, the adapter fill-in step involved *Bst* DNA Polymerase (NEB) at 37°C for 30 minutes, followed by heat inactivation of 20 minutes at 80°C. Dual-indexing amplifications were set up using AmpliTaq Gold (5U/µl), Thermopol

reaction buffer (10x), dNTPs (10mM each), both indexing primers (10µM each) and 10µl DNA sample library. The following thermal cycling steps were used for amplification: 12 minutes at 95°C, followed by 10 cycles of 20 seconds at 95°C, 30 seconds at 60°C and 40 seconds at 72°C, and then a final extension step of 5 min at 72°C. The amplification product was purified using the QIAQuick kit.

For the second amplification round, Accuprime *Pfx* Supermix (Life Technology) was used, together with primers IS5 (10µM), IS6 (10µM) and 2.5µl of sample library. Amplification took place under the following thermal cycling conditions: 30 seconds at 98°C, followed by 10 cycles of 20 seconds at 98°C, 30 seconds at 60°C and 40 seconds at 72°C, and then a final extension of 5 minutes at 72°C. The amplification products were purified as described above, and quantified using a Qubit 3.0 Fluorometer, before quantifying the libraries using an Agilent 2100 Bioanalyzer High Sensitivity DNA kit in order to pool them together in an equimolar solution. NGS libraries were sequenced on an Illumina HiSeq2500 (1 × 100bp) by NBAF Liverpool.

Data processing and read mapping

The NGS reads were trimmed using cutadapt (v.1.13; Martin 2011), allowing a minimum overlap of 1 base pair (bp) between read and adapter (adapter sequence: AGATCGGAAGAGCACACGTCTGAACTCCAGTCAC), and discarding reads shorter than 30bp. BWA aln (v. 0.7.12-r1039; Li & Durbin 2009) was used to map reads to both the human mitochondrial genome (rCRS) and the human reference genome (UCSC hg19), filtering by base quality 15, and disabling seed length as recommended for ancient DNA data (Schubert *et al*. 2012). Samtools (v.1.3) was used to sort and filter reads, and to remove amplification duplicates.

Ancient DNA authenticity

To assess the anti-contamination measures described above, negative controls were introduced during each stage of sample processing. An air control and a water control were included at the drilling and powdering stage. The air control consisted of an empty 1.5ml Eppendorf tube, which was placed for one hour with an open lid in the cleaned work area between sample processing. For the water control, 2ml of ddH_2O was shaken with a steel ball inside a metal shaker in a Mixer Mill (Retsch MM400). 1ml of the water control was then taken through the complete extraction protocol. Controls introduced during the extraction process were quantified using a Qubit 3.0 Fluorometer. Negative controls from the extraction,

the USER treatment, and the amplification step (×2) were sequenced alongside the three sample libraries on an Illumina HiSeq2500, using 100bp single-end reads.

The two main patterns of typical ancient DNA post-mortem degradation – over-representation of C to T changes at the end of reads, and short sequence length – were assessed using mapDamage 2.0 (Jónsson *et al*. 2013) and bamdamage (Malaspinas *et al*. 2014). Reads were only taken into account if they had a minimum mapping quality of 30.

Genetic sexing and mitochondrial haplotype calling

To determine the sex of the analysed ancient sample, a software was used that calculates the ratio of reads aligning to the X and Y chromosome reads from the whole genome dataset (Skoglund *et al*. 2013). The mitochondrial haplotype was determined by aligning the sequence reads to the revised Cambridge Reference Sequence (rCRS, NC_012920; Andrews *et al*. 1999), using BWA aln filtering (with -b and -q 30) and removal of duplicate reads. The mtDNA consensus sequence was called using Samtools mpileup, as in Martiniano *et al*. (2016). Haplofind (Vianello *et al*. 2013) was used to identify haplogroup defining mutations and assign the haplogroup of the sample. The mtDNA coverage was estimated using EAGER (Peltzer *et al*. 2016).

Results

The DNA content of all the controls introduced during the extraction process was too low to be measured. Amplification reactions were quantified using a Qubit 3.0 Fluorometer (Table S5).

Table S5. Qubit measurements of the sequencing libraries.

ID	DNA concentration (ng/µl)
USER blank	1.40
Sample Library 1	6.74
Sample Library 2	14.00
Sample Library 3	4.73
Amplification blank	0.88
Negative control library	0.99
Amplification blank	0.81

The contamination of all control samples was estimated to be lower than 0.5% (Gamba *et al*. 2014). The program schmutzi (Renaud *et al*. 2015) was used to detect introduction of modern mitochondrial contamination in the sample, with estimates ranging from 0.12% to 0.17%, which is very low. The two main patterns of post-mortem degradation were assessed and the reads from the sample showed an increase in C to T and G to A transitions towards the 5' and 3' ends, which are characteristic changes of ancient molecules (Briggs *et al*. 2007; Brotherton *et al*. 2007). Although many sequences had a length of 100bp, this was inflated as the sample was sequenced using 100bp single-end sequencing. Sequences greater than 100bp were truncated but, in keeping with the DNA being from an ancient source, the average sequence length was less than 100bp. The NGS sequencing results are displayed in Table S6.

Table S6. Next-generation sequencing results for the Oakridge individual.

Genome coverage	1.0143x
Contamination estimate	0.145% (0.12-0.17)
Mean mapping quality	12.029
GC content in %	45.61
Number of mapped reads	65,698,100
Number of mapped bases	3,260,000,000
Duplication rate	2.67%

The endogenous DNA content retrieved from the sample was calculated to be 70.08%. The ratio of reads aligning to the X and Y chromosome allowed an unambiguous classification of the sample as genetically female (XX) (Table S7).

Table S7. Molecular sex assignment of the Oakridge individual.

Ry	Standard error	95% confidence interval	Assignment
0.0023	0	0.0022-0.0024	female

The coverage of the mitochondrial genome was over 42x, and the individual was found to have all the defining mutations of haplogroup H3g1a (Table S8).

Table S8. Mitochondrial haplogroup and haplotype for the Oakridge individual.

Coverage	Haplogroup	Haplotype
42.29x	H3g1a	152C 263G 750G 1438G 2523Y 3992T 4135C 4418C 4769G 6776C 8251A 8860G 10754C 15326G 15377G 16519C

Discussion

As morphological indicators were unable to identify the sex of the Oakridge individual (mainly due to partial remains and young age of the individual), the sex was determined genetically. From extracting and analysing the DNA, the person was found to be female. She had a mitochondrial haplotype of H3g1a. Today, over 40% of all maternal lineages in Europe belong to haplogroup H. H3 has high frequency in modern-day Spain (Achilli *et al*. 2004) and in the Western Isles of Scotland (Brotherton *et al*. 2013), and is also present in the middle Neolithic period (including at Orkney) and the Bell Beaker culture in Europe (Brotherton *et al*. 2013; Olalde *et al*. 2018). H3g1 is generally seen in modern-day north-western European people, with the root comprising solely of people from Denmark (data not shown), although English, Scottish, Welsh, German and Dutch people also group within the H3g1 clade. Unfortunately, nothing can be said about the origin of the female based on her maternal lineage. Looking at the nuclear DNA, the Oakridge specimen falls within the pattern of genetic variation seen amongst other post-Roman and Anglo-Saxon individuals that have been analysed from elsewhere in Britain. There is no evidence of African genetic input in this individual.

References

ACHILLI, A. *et al*. 2004. The molecular dissection of mtDNA haplogroup H confirms that the Franco-Cantabrian glacial refuge was a major source for the European gene pool. *American Journal of Human Genetics* 75: 910–18.

AL QAHTANI, S.J. 2008. *Atlas of tooth development and eruption*. London: Queen Mary University of London.

AL QAHTANI S.J., M.P. HECTOR & H.M. LIVERSIDGE. 2014. Accuracy of dental age estimation charts: Schour and Massler, Ubelaker and the London Atlas. *American Journal of Physical Anthropology* 154: 70–78. https://doi.org/10.1002/ajpa.22473

ALHAZMI, A., E. VARGAS J.M. PALOMO, M. HANS, B. LATIMER & S. SIMPSON. 2017. Timing and rate of spheno-occipital synchondrosis closure and its relationship to puberty. *PloS One* 12: e0183305–e0183305. https://doi.org/10.1371/journal.pone.0183305

ANDREWS, R.M., I. KUBACKA, P.F. CHINNERY, R.N. LIGHTOWLERS, D.M. TURNBULL & N. HOWELL. 1999. Reanalysis and revision of the Cambridge reference sequence for human mitochondrial DNA. *Nature Genetics* 23: 147. https://doi.org/10.1038/13779

BENTLEY, R.A. 2006. Strontium isotopes from the earth to the archaeological skeleton: a review. *Journal of Archaeological Method and Theory* 13: 135–87. https://doi.org/10.1007/s10816-006-9009-x

BRIGGS, A.W. *et al*. 2007. Patterns of damage in genomic DNA sequences from a Neandertal. *Proceedings of the National Academy of Sciences of the USA* 104: 14616–21. https://doi.org/10.1073/pnas.0704665104

BROCA, P. 1868. On the crania and bones of Les Eyzies, Dordogne. *Transactions of the International Congress of Prehistoric Archaeology* 3: 168–75.

BRONK RAMSEY, C. 2017. Methods for summarizing radiocarbon datasets. *Radiocarbon* 59: 1809–33. https://doi.org/10.1017/RDC.2017.108

BRONK RAMSEY, C., T.G.F. HIGHAM, D.C. OWEN, A.W.G. PIKE & R.E.M. HEDGES. 2002. Radiocarbon dates from the Oxford AMS System: Archaeometry Datelist 31. *Archaeometry* 44 (Supplement 1): 1–150. https://doi.org/10.1111/j.1475-4754.2002.tb01101.x

BRONK RAMSEY, C., T. HIGHAM & P. LEACH. 2004a. Towards high-precision AMS: progress and limitations. *Radiocarbon* 46: 17–24. https://doi.org/10.1017/S0033822200039308

BRONK RAMSEY, C., T.G.F. HIGHAM, A. BOWLES & R. HEDGES. 2004b. Improvements to the pretreatment of bone at Oxford. *Radiocarbon* 46: 155–63. https://doi.org/10.1017/S0033822200039473

BROTHERTON, P., P. ENDICOTT, J.J. SANCHEZ, M. BEAUMONT, R. BARNETT, J. AUSTIN & A. COOPER. 2007. Novel high-resolution characterization of ancient DNA reveals C > U-type base modification events as the sole cause of post mortem miscoding lesions. *Nucleic Acids Research* 35: 5717–28. https://doi.org/10.1093/nar/gkm588

BROTHERTON, P. *et al*. 2013. Neolithic mitochondrial haplogroup H genomes and the genetic origins of Europeans. *Nature Communications* 4: 1764. https://doi.org/10.1038/ncomms2656

BRYANT, J.D., P.L. KOCH, P.N. FROELICH, W.J. SHOWERS & B.J. GENNA. 1996. Oxygen isotope partitioning between phosphate and carbonate in mammalian apatite. *Geochimica et Cosmochim Acta* 60: 5145–48. https://doi.org/10.1016/S0016-7037(96)00308-0

BUIKSTRA, J.E. & D.H. UBELAKER. 1994. *Standards for data collection from human skeletal remains* (Arkansas Archeological Survey research series, no. 44). Fayetteville: Arkansas Archaeological Society.

CHENERY, C., G. MÜLDNER, J. EVANS, H. ECKARDT & M. LEWIS. 2010. Strontium and stable isotope evidence for diet and mobility in Roman Gloucester, UK. *Journal of Archaeological Science* 37: 150–63. https://doi.org/10.1016/j.jas.2009.09.025

COHEN, A.S., R.K. ONIONS, R. SIEGENTHALER & W.L. GRIFFIN. 1988. Chronology of the pressure-temperature history recorded by a granulite terrain. *Contributions to Mineralogy and Petrology* 98: 303–11. https://doi.org/10.1007/BF00375181

DARLING, W.G. & J.C. TALBOT. 2003. The O & H stable isotopic composition of fresh waters in the British Isles: 1. Rainfall. *Hydrology and Earth System Sciences B* 7: 163–81. https://doi.org/10.5194/hess-7-163-2003

ELLIOTT, M. & M. COLLARD. 2009. Fordisc and the determination of ancestry from cranial measurements. *Biology Letters* 5: 849–52. https://doi.org/10.1098/rsbl.2009.0462

EVANS, J.A., J. MONTGOMERY, G. WILDMAN & N. BOULTON. 2010. Spatial variations in biosphere $^{87}Sr/^{86}Sr$ in Britain. *Journal of the Geological Society* 167: 1–4. https://doi.org/10.1144/0016-76492009-090

FEREMBACH, D., I. SCHWINDEZKY & M. STOUKAL. 1980. Recommendations for age and sex diagnoses of skeletons. *Journal of Human Evolution* 9: 517–49. https://doi.org/10.1016/0047-2484(80)90061-5

GAMBA, C. *et al.* 2014. Genome flux and stasis in a five millennium transect of European prehistory. *Nature Communications* 5: 5257. https://doi.org/10.1038/ncomms6257

HOWELLS, W.W. 1973. *Cranial variation in man: a study by multivariate analysis of patterns of difference among recent human populations*. Cambridge (MA): Harvard University Press.

– 1989. *Skull shapes and the map: craniometric analyses in the dispersion of modern Homo*. Cambridge (MA): Harvard University Press.

HULL, B.D. 2008. Social differentiation and diet in Early Anglo-Saxon England: stable isotope analysis of archaeological human and animal remains. Unpublished PhD dissertation, University of Oxford.

JANTZ, R.L. & S.D. OUSLEY. 2005. *FORDISC 3: computerized forensic discriminant functions* (version 3.1). Knoxville: University of Tennessee.

JÓNSSON, H.A. GINOLHAC, M. SCHUBERT, P.L. JOHNSON & L. ORLANDO. 2013. MapDamage2.0: fast approximate Bayesian estimates of ancient DNA damage parameters. *Bioinformatics* 29: 1682–84. https://doi.org/10.1093/bioinformatics/btt193

KIM, S.-T., T.B. COPLEN & J. HORITA. 2015. Normalization of stable isotope data for carbonate minerals: implementation of IUPAC guidelines. *Geochimica et Cosmochimica Acta* 158: 276–89. https://doi.org/10.1016/j.gca.2015.02.011

KING, J. & G. COLE. 2016. The radiocarbon dating of human remains from seven sites in north Hampshire, with special reference to the results from Old Basing. *Proceedings of the Hampshire Field Club and Archaeological Society* 71: 76–88.

KIRCHER, M., S. SAWYER & M. MEYER. 2012. Double indexing overcomes inaccuracies in multiplex sequencing on the Illumina platform. *Nucleic Acids Research* 40: e3. https://doi.org/10.1093/nar/gkr771

KNÜSEL, C.J. & G.C. CARR. 1995. On the significance of the crania from the River Thames and its tributaries, with comment by Richard Bradley. *Antiquity* 69: 162. https://doi.org/10.1017/S0003598X00064395

LEVINSON, A.A., B. LUZ & Y. KOLODNY. 1987. Variations in oxygen isotopic compositions of human teeth and urinary stones. *Applied Geochemistry Frontiers in Analytical Geochemistry-an IGC 2004 Perspective* 2: 367–71. https://doi.org/10.1016/0883-2927(87)90021-7

LEWIS, J.E. 2008. Identifying sword marks on bone: criteria for distinguishing between cut marks made by different classes of bladed weapons. *Journal of Archaeological Science* 35: 2001–2008. https://doi.org/10.1016/j.jas.2008.01.016

LI, H. & R. DURBIN. 2009. Fast and accurate short read alignment with Burrows-Wheeler transform. *Bioinformatics* 25: 1754–60. https://doi.org/10.1093/bioinformatics/btp324

MACHUGH, D.E., C.J. EDWARDS, J.F. BAILEY, D.R. BANCROFT & D.G. BRADLEY. 2000. The extraction and analysis of ancient DNA from bone and teeth: a survey of current methodologies. *Ancient Biomolecules* 3: 81–102.

MALASPINAS, A.S. *et al*. 2014. Bammds: a tool for assessing the ancestry of low-depth whole genome data using multidimensional scaling (MDS). *Bioinformatics* 30: 2962–64. https://doi.org/10.1093/bioinformatics/btu410

MARTIN, M. 2011. Cutadapt removes adapter sequences from high-throughput sequencing reads. *EMBnet.journal* 17: 10. https://doi.org/10.14806/ej.17.1.200

MARTINIANO, R., C. COELHO, M.T. FERREIRA, M.J. NEVES, R. PINHASI & D.G. BRADLEY. 2014. Genetic evidence of African slavery at the beginning of the trans-Atlantic slave trade. *Scientific Reports* 4: 5994. https://doi.org/10.1038/srep05994

MARTINIANO, R. *et al*. 2016. Genomic signals of migration and continuity in Britain before the Anglo-Saxons. *Nature Communications* 7: 10326. https://doi.org/10.1038/ncomms10326

MEYER, M. & M. KIRCHER. 2010. Illumina sequencing library preparation for highly multiplexed target capture and sequencing. *Cold Spring Harbor Protocols* 6: 5448. https://doi.org/10.1101/pdb.prot5448

MÍKOVÁ, J. & P. DENKOVÁ. 2007. Modified chromatographic separation scheme for Sr and Nd isotope analysis in geological silicate samples. *Journal of Geosciences* 52: 221–26. https://doi.org/10.3190/jgeosci.015

MILES, A.E.W. 1962. Assessment of the ages of a population of Anglo-Saxons from their dentition. *Proceedings of the Royal Society of Medicine* 55: 881–86. https://doi.org/10.1177/003591576205501019

MOORREES, C.F.A., E.A. FANNING & E.E. HUNT, JR. 1963. Age variation of formation stages for ten permanent teeth. *Journal of Dental Research* 42: 1490–1502. https://doi.org/10.1177/00220345630420062701

OLALDE, I. *et al*. 2018. The Beaker phenomenon and the genomic transformation of northwest Europe. *Nature* 555: 190–96. https://doi.org/10.1038/nature25738

PELTZER, A., G. JÄGER, A. HERBIG, A. SEITZ, C. KNIEP, J. KRAUSE & K. NIESELT. 2016. EAGER: efficient ancient genome reconstruction. *Genome Biology* 17: 60. https://doi.org/10.1186/s13059-016-0918-z

PIN, C., D. BRIOT, C. BASSIN & F. POITRASSON. 1994. Concomitant separation of strontium and samarium-neodymium for isotopic analysis in silicate samples, based on specific extraction chromatography. *Analytica Chimica Acta* 298: 209–17. https://doi.org/10.1016/0003-2670(94)00274-6

POLLARD A.M. & C. HERON. 2008. *Archaeological chemistry*. 2nd edition. Cambridge: Royal Society of Chemistry.

POLLARD, A.M., M. PELLEGRINI & J.A. LEE-THORP. 2011. Technical note: some observations on the conversion of dental enamel $\delta^{18}O(p)$ values to $\delta^{18}O(w)$ to determine human mobility. *American Journal of Physical Anthropology* 145: 499–504. https://doi.org/10.1002/ajpa.21524

RAMSTHALER, F., K. KREUTZ & M. VERHOFF. 2007. Accuracy of metric sex analysis of skeletal remains using Fordisc® based on a recent skull collection *International Journal of Legal Medicine* 121: 477–82. https://doi.org/10.1007/s00414-007-0199-x

REIMER, P.J. *et al*. 2013. IntCal13 and Marine13 radiocarbon age calibration curves 0–50 000 years cal BP. *Radiocarbon* 55: 1869–87. https://doi.org/10.2458/azu_js_rc.55.16947

RENAUD, G., V. SLON, A.T. DUGGAN & J. KELSO. 2015. Schmutzi: estimation of contamination and endogenous mitochondrial consensus calling for ancient DNA. *Genome Biology* 16: 224. https://doi.org/10.1186/s13059-015-0776-0

SAUNDERS, S., C. DEVITO, A. HERRING, R. SOUTHERN & R. HOPPA. 1993. Accuracy tests of tooth formation age estimations for human skeletal remains. *American Journal of Physical Anthropology* 92: 173–88. https://doi.org/10.1002/ajpa.1330920207

SCHUBERT M., A. GINOLHAC, S. LINDGREEN, J.F. THOMPSON, K.A.S. AL-RASHEID, E. WILLERSLEV, A. KROGH & L. ORLANDO. 2012. Improving ancient DNA read mapping

against modern reference genomes. *BMC Genomics* 13: 178. https://doi.org/10.1186/1471-2164-13-178

SKOGLUND, P. J. STORÅ, A. GÖTHERSTRÖM & M. JAKOBSSON. 2013. Accurate sex identification of ancient human remains using DNA shotgun sequencing. *Journal of Archaeological Science* 40: 4477–82. https://doi.org/10.1016/j.jas.2013.07.004

VAN KLINKEN, G.J. 1999. Bone collagen quality indicators for palaeodietary and radio carbon measurements. *Journal of Archaeological Science* 26: 687–95. https://doi.org/10.1006/jasc.1998.0385

VIANELLO, D., F. SEVINI, G. CASTELLANI, L. LOMARTIRE, M. CAPRI & C. FRANCESCHI. 2013. HAPLOFIND: a new method for high-throughput mtDNA haplogroup assignment. *Human Mutation* 34: 1189–94. https://doi.org/10.1002/humu.22356

YANG, D.Y., B. ENG, J.S. WAYE, J.C. DUDAR & S.R. SAUNDERS. 1998. Technical note: improved DNA extraction from ancient bones using silica-based spin columns. *American Journal of Physical Anthropology* 105: 539–43. https://doi.org/10.1002/(SICI)1096-8644(199804)105:4<539::AID-AJPA10>3.0.CO;2-1